A Theory of Asymmetric Hypersonic Blunt-Body Flows

RUDOLPH J. SWIGART*
Lockheed Missiles and Space Company, Palo Alto, Calif.

Two-dimensional asymmetric and three-dimensional inviscid blunt-body flows are analyzed using a new method. The method is inverse, that is, the shock-wave shape and freestream conditions are taken as known, and the body shape and flow field are to be determined. Results at zero angle of attack are obtained as a special case of the general problem. Solutions at zero angle are calculated for a variety of body shapes at freestream Mach numbers ranging from infinity to 1.85. The ratio of specific heats, γ, is taken as 1.4. Comparison with results obtained using Van Dyke's and Garabedian's numerical solutions indicates that the method under consideration is more accurate than the Van Dyke method for determining stand-off distance. Solutions are obtained for parabolic and paraboloidal shock waves at small angle of attack and infinite freestream Mach number; γ assumes the values 1.4, 1.2, 1.1, and 1.05. For all cases, the streamline that wets the body passes through the shock wave slightly above the point where the shock is normal and thus does not possess maximum entropy. These results provide counter examples to the conjecture that any isolated convex body in a supersonic stream is wetted by the streamline of maximum entropy.

I. Introduction

FOR more than a decade, theoreticians interested in high-speed gasdynamics have been seeking a solution to the blunt-body problem that combines the advantages of minimum computational difficulty with maximum accuracy of results. Physically, the problem under consideration is the following. A blunt-nosed configuration is traveling through a uniform gas at a flight Mach number greater than unity. A detached shock wave forms ahead of the body at a position depending on the body shape, flight direction and Mach number, and certain physical properties of the gas. The gas ahead of the shock wave is unaffected by the presence of the body. It is desired to determine the flow properties (e.g., velocity, pressure, density) in the region between the shock and the body. In general, this region may be divided into two subregions, depending on the magnitude of the local flow Mach number with respect to unity. The locus of points at which the local flow Mach number is unity is called the sonic line. If one considers steady flow relative to the body and denotes by M and M_l the freestream and local Mach numbers, respectively, then an example of the foregoing situation is depicted in Fig. 1.

Mathematically, the problem considered is governed by highly nonlinear differential equations in a domain possessing a free boundary along which initial values may be determined if the boundary shape and freestream conditions are known. The governing equations are of elliptic type in the subsonic region ($M_l < 1$) and of hyperbolic type in the supersonic region ($M_l > 1$). The initial-value problem for hyperbolic equations is well posed and yields to solution using the well-known theory of characteristics. The initial-value problem for elliptic equations, however, is posed poorly, and much of the effort expended on the blunt-body problem has been confined to its solution in the subsonic region. Attempts have been made to solve the problem by both inverse and direct methods. In the inverse method, the shape of the detached shock and the freestream conditions are prescribed, and the corresponding body shape and flow field are to be determined. In the direct method, the body shape and freestream conditions are prescribed, and the corresponding shock-wave shape and flow field are to be determined. References 1 and 2 contain detailed reviews of and extensive references to previous work for plane-symmetric and axisymmetric shapes at zero angle of attack, i.e., bodies whose flight direction is parallel to the body axis of symmetry.

The methods now in popular use for solving the zero-angle problem in the entire subsonic region to a high degree of accuracy are numerical in nature and require the use of high-speed electronic computing machines. Two such methods are Van Dyke's[3] approach to the inverse problem and Belotserkovskii's[4] solution to the direct problem. Van Dyke's analysis essentially reduces the solution of the conservation equations for steady, inviscid flow of a perfect, non-heat-conducting gas to numerical integration of two coupled partial differential equations for the density and stream function. Belotserkovskii, on the other hand, by assuming a polynomial variation between the shock and body for certain flow quantities, reduces the problem to integration of ordinary differential equations. Practical experience has shown that both of these methods require a large amount of skill on the part of the numerical analyst in order to obtain satisfactory solutions for other than simple body shapes such as spheres or circular cylinders. Hence, even though these methods yield fairly high accuracy, they possess a moderate amount of computational difficulty.

In contrast to the zero-angle problem, comparatively little effort has been expended on the problem of the blunt body at angle of attack in either the two-dimensional or three-dimensional cases. Both Mangler[5] and Vaglio-Laurin and Ferri[6] suggest computational methods for attacking such problems, but neither presents results using the analyses proposed. They both obtain solutions to the zero-angle inverse problem by introducing the stream function as an independent variable through a von Mises transformation. The resulting partial differential equations are then numerically integrated from the shock to the body using a marching technique. Mangler suggests an extension of this marching technique to the three-

Presented at the IAS Annual Summer Meeting, Los Angeles, Calif., June 19–22, 1962; revision received March 6, 1963. The author expresses his gratitude to Milton D. Van Dyke of Stanford University for his many technical contributions to the development of the theory, to Martin J. Lanfranco of Lockheed Missiles and Space Company for performing the algebra and carrying out the programming for the finite Mach number, zero angle cases, and to Helen Kirch and Ann Campbell of Lockheed Missiles and Space Company for their aid in reducing the data. The infinite Mach number portion of this work was carried out as part of Contract No. AF 49(638)-965, monitored by the Air Force Office of Scientific Research of the Air Research and Development Command.

* Associate Research Scientist, Mathematical and Mechanical Sciences Laboratory.

dimensional angle-of-attack problem formulated in terms of a pair of stream functions. The approach of Vaglio-Laurin and Ferri to the problem of the blunt body at incidence involves a first-order perturbation of the flow variables about their zero-angle values.

Vaglio-Laurin[7] has developed another approach to the blunt-body problem at zero or finite incidence which involves the successive refinement of an approximate solution by application of the PLK method. Results for configurations at both zero and finite angle of attack using the analysis are presented in Ref. 7.

The success, however, of Mangler's and Vaglio-Laurin's methods for the solution of the angle-of-attack problem depends on an assumption regarding a basic property of asymmetric supersonic flows. The assumption is that the body is covered by the streamline that crosses the shock at right angles and thus possesses maximum entropy in the flow between the shock wave and body. Mangler has conjectured that such a condition might be a feature of any flow, whereas Vaglio-Laurin (Ref. 7, p. 19) purportedly has proven this to be true for two-dimensional asymmetric configurations. However, the proof has been found to be faulty, and Vaglio-Laurin is in accord with this conclusion.[17]

The analysis that follows yields solutions for two- and three-dimensional supersonic and hypersonic flow past blunt bodies at small angles of incidence. The method is an inverse one, that is, the shock-wave shape, freestream conditions, and angle of incidence of the shock wave are known, and the corresponding body and flow field are to be obtained. The equations of motion are solved using a semi-analytical, semi-numerical approach that reduces the problem to numerical integration of ordinary differential equations. The solution may be carried to any desired degree of accuracy and requires no extensive numerical analytical skill. Moreover, no assumption need be made regarding the behavior of the maximum-entropy streamline. Its position in the flow is obtained as part of the solution. Results at zero incidence are obtained as a special case of the general problem. Although the examples chosen are for specific shock shapes and, in the majority of cases, a specific-heat ratio of 1.4, the analysis is performed for the general case. The method of extension to higher angles is obvious and introduces no new difficulties.

II. Analysis

A. Coordinate System

The coordinate system adopted is that developed by Van Dyke.[3] The detached shock wave is described by a conic section so that it is a portion of a hyperboloid of revolution, paraboloid, prolate ellipsoid, sphere, or oblate ellipsoid. In cylindrical polar coordinates originating from its vertex, any such shock has the equation

$$r^2 = 2R_s x - Bx^2 \tag{1}$$

where R_s is the nose radius of the shock and B is a parameter characterizing the eccentricity of the conic section; B is negative for hyperboloids, zero for paraboloids, positive for ellipsoids, and unity for a sphere.

An orthogonal coordinate system (ξ,η) that contains the shock wave as a coordinate surface is defined by

$$x/R_s = (1/B)\{1 - [(1 - B\xi^2)(1 - B + B\eta^2)]^{1/2}\} \tag{2a}$$

$$r/R_s = \xi\eta \tag{2b}$$

Special cases are, for the parabola ($B = 0$),

$$x/R_s = \tfrac{1}{2}(1 + \xi^2 - \eta^2) \tag{2c}$$

and for the circle ($B = 1$),

$$x/R_s = 1 - \eta(1 - \xi^2)^{1/2} \tag{2d}$$

The shock wave is described by $\eta = 1$.

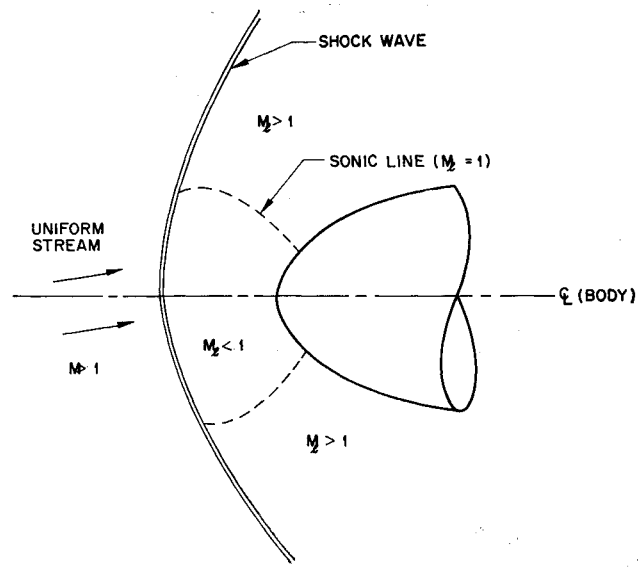

Fig. 1 Flow-field characteristics of a blunt body in hypersonic flight

In this coordinate system, with the azimuthal angle φ as the third orthogonal coordinate, the differential line element ds is given by

$$ds^2 = h_1^2 d\xi^2 + h_2^2 d\eta^2 + h_3^2 d\varphi^2$$
$$\equiv \left(\frac{C\xi^2 + \eta^2}{1 - B\xi^2}\, d\xi^2 + \frac{C\xi^2 + \eta^2}{C + B\eta^2}\, d\eta^2 + \nu\xi^2\eta^2 d\varphi^2\right) R_s^2 \tag{3}$$

where $C = 1 - B$. Here ν is a geometric parameter, being 0 for plane and 1 for axisymmetric or three-dimensional flow.

B. Differential Equations, Initial Conditions, and Method of Solution

Denote by $\mathbf{q}$, ρ, and p the velocity, density, and pressure nondimensionalized with respect to the freestream speed q_∞, the freestream density ρ_∞, and twice the freestream dynamic pressure $\rho_\infty q_\infty^2$, respectively. Then, the equations expressing conservation of mass, momentum, and entropy for steady inviscid flow of a perfect, non-heat-conducting gas having constant specific heats are

$$\nabla\cdot(\rho\mathbf{q}) = 0 \tag{4a}$$

$$\rho\mathbf{q}\cdot\nabla\mathbf{q} + \nabla p = 0 \tag{4b}$$

$$\mathbf{q}\cdot\nabla(p/\rho^\gamma) = 0 \tag{4c}$$

where γ is the adiabatic exponent.

One sets $R_s = 1$ without loss of generality. Equations (4a–4c) become, in (ξ,η,φ) coordinates,

$$\left[(\xi\eta)^\nu\left(\frac{C\xi^2 + \eta^2}{C + B\eta^2}\right)^{1/2}\rho u\right]_\xi + \left[(\xi\eta)^\nu\left(\frac{C\xi^2 + \eta^2}{1 - B\xi^2}\right)^{1/2}\rho v\right]_\eta + \left\{\frac{C\xi^2 + \eta^2}{[(1 - B\xi^2)(C + B\eta^2)]^{1/2}}\rho w\right\}_\varphi = 0 \tag{5a}$$

$$\rho\left[uu_\xi - \frac{C\xi v^2}{C\xi^2 + \eta^2} + \left(\frac{C + B\eta^2}{1 - B\xi^2}\right)^{1/2} v\left(u_\eta + \frac{\eta u}{C\xi^2 + \eta^2}\right) + \frac{w}{\xi\eta}\left(\frac{C\xi^2 + \eta^2}{1 - B\xi^2}\right)^{1/2} u_\varphi - \frac{w^2}{\xi}\right] + p_\xi = 0 \tag{5b}$$

$$\rho\left[vv_\eta - \frac{\eta u^2}{C\xi^2 + \eta^2} + \left(\frac{1 - B\xi^2}{C + B\eta^2}\right)^{1/2} u\left(v_\xi + \frac{C\xi v}{C\xi^2 + \eta^2}\right) + \frac{w}{\xi\eta}\left(\frac{C\xi^2 + \eta^2}{C + B\eta^2}\right)^{1/2} v_\varphi - \frac{w^2}{\eta}\right] + p_\eta = 0 \tag{5c}$$

$$\rho\left[ww_\varphi + u\eta\left(\frac{1-B\xi^2}{C\xi^2+\eta^2}\right)^{1/2}(w+\xi w_\xi) + v\xi\left(\frac{C+B\eta^2}{C\xi^2+\eta^2}\right)^{1/2}(w+\eta w_\eta)\right] + p_\varphi = 0 \quad (5d)$$

$$u\left(\frac{1-B\xi^2}{C\xi^2+\eta^2}\right)^{1/2}\left(\frac{p}{\rho^\gamma}\right)_\xi + v\left(\frac{C+B\eta^2}{C\xi^2+\eta^2}\right)^{1/2}\left(\frac{p}{\rho^\gamma}\right)_\eta + \frac{w}{\xi\eta}\left(\frac{p}{\rho^\gamma}\right)_\varphi = 0 \quad (5e)$$

Here u,v, and w are the components of $\mathbf{q}$ in the ξ,η, and φ directions, and subscripts ξ,η, and φ denote partial differentiation in the usual sense.

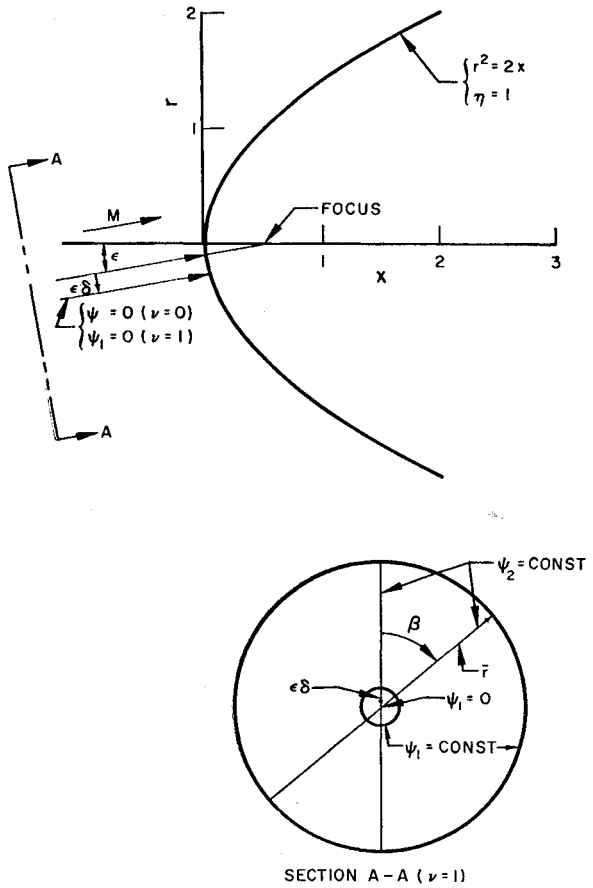

Fig. 2 Parabolic or paraboloidal shock wave at angle of attack

Since the method of solution varies slightly between the two- and three-dimensional cases, departure will now be taken from a concurrent treatment.

1. *Plane flow*

Equations (5a–5e) apply with $\nu = w = \partial/\partial\varphi = 0$. The first (continuity) equation is satisfied by introducing a stream function defined by

$$\psi_\eta = \left(\frac{C\xi^2+\eta^2}{C+B\eta^2}\right)^{1/2}\rho u \qquad \psi_\xi = -\left(\frac{C\xi^2+\eta^2}{1-B\xi^2}\right)^{1/2}\rho v \quad (6)$$

Then the last (entropy) equation simply states that

$$p = \rho^\gamma f(\psi) \quad (7)$$

where the functional form of f is determined by the boundary conditions at the shock. Using Eq. (7) to eliminate the pressure from the equations of motion yields

$$\left[\gamma\frac{C\xi^2+\eta^2}{1-B\xi^2}f\rho^{\gamma+1} - \psi_\xi^2\right]\frac{\rho_\eta}{\rho} = \psi_\eta\psi_{\xi\xi} + \frac{\eta}{C\xi^2+\eta^2}\left(\psi_\xi^2 + \frac{C+B\eta^2}{1-B\xi^2}\psi_\eta^2\right) - \psi_\xi\psi_{\xi\eta} - \psi_\xi\psi_\eta\frac{\rho_\xi}{\rho} - \frac{B\xi}{1-B\xi^2}\psi_\xi\psi_\eta - \frac{C\xi^2+\eta^2}{1-B\xi^2}\rho^{\gamma+1}f'\psi_\eta \quad (8a)$$

$$\psi_\xi\psi_{\eta\eta} = \psi_\eta\psi_{\xi\eta} + \psi_\eta\left(\psi_\xi\frac{\rho_\eta}{\rho} - \psi_\eta\frac{\rho_\xi}{\rho}\right) - \frac{C\xi}{C\xi^2+\eta^2}\left(\frac{1-B\xi^2}{C+B\eta^2}\psi_\xi^2 + \psi_\eta^2\right) - \frac{B\eta}{C+B\eta^2}\psi_\xi\psi_\eta + \frac{C\xi^2+\eta^2}{C+B\eta^2}f\rho^{\gamma+1}\left(\gamma\frac{\rho_\xi}{\rho} + \frac{f'}{f}\psi_\xi\right) \quad (8b)$$

where f' denotes the derivative of f with respect to its argument.

Thus far, the attitude of the body with respect to the freestream, or, since the inverse problem is being considered, the angle of the uniform freestream with the shock axis of symmetry has not entered into the mathematical formulation. The angle of attack of the shock will, however, appear in the boundary conditions and in the explicit expression for $f(\psi)$. These conditions will be derived by employing McLaurin series expansions about zero angle of attack and retaining first-order terms in shock angle of attack, ϵ. Setting ϵ equal to zero recovers the zero-angle conditions.

Moreover, in the angle-of-attack problem, the position in the flow ahead of the shock wave of the streamline that wets the body is not known a priori but must be obtained as part of the solution. A fundamental question in the analysis of hypersonic flows past inclined blunt bodies concerns the behavior of this streamline. It has been conjectured[5, 7] that any isolated convex body in a uniform supersonic stream is covered by the fluid of maximum entropy in the flow. This means that the stagnation streamline must have crossed the bow shock where it is a normal shock wave. To determine the position of the stagnation streamline in the freestream and thus possibly disprove the conjecture, the formulation of the angle-of-attack problem requires the introduction of an additional parameter δ (Fig. 2). The quantity δ is a measure of the distance of the body streamline in the freestream from a given reference line. This reference line is at angle ϵ to the x axis and, in general, is taken to pass through the point $x/R_s = 1/B$, $r/R_s = 0$. However, in the singular case of the parabola ($B = 0$), the reference line is taken through the focus of the parabola ($x/R_s = \frac{1}{2}$, $r/R_s = 0$).

Values of u,v,p,ρ just behind the shock wave ($\eta = 1$) are found from the oblique shock relations (e.g., Ref. 8) in terms of the angle that the tangent to the bow wave makes with the freestream direction. Expressing this angle in terms of the slope of the bow wave, $(1 - B\xi^2)^{1/2}/B$ and ϵ, using Eqs. (6), and retaining first-order terms in ϵ results in the initial conditions

$$\rho = \frac{(\gamma+1)M^2[1-B\xi^2-2\epsilon\xi(1-B\xi^2)^{1/2}]}{(\gamma-1)M^2[1-B\xi^2-2\epsilon\xi(1-B\xi^2)^{1/2}]+2(1+C\xi^2)}$$

$$\psi = \xi + \epsilon\left[\frac{(1-B\xi^2)^{1/2}}{B} + \delta\right] \qquad \psi_\eta = \rho[\xi + \epsilon(1-B\xi^2)^{1/2}] \qquad \text{at } \eta = 1 \quad (9a)$$

and gives for the function $f(\psi)$

$$f(\psi) = \frac{2\gamma M^2(1 - B\psi^2 + 2\epsilon B\psi\delta) - (\gamma - 1)[1 + C\psi^2 - 2\epsilon C\psi\{[(1 - B\xi^2)^{1/2}/B] + \delta\}]}{\gamma(\gamma + 1)M^2\{1 + C[\psi^2 - 2\epsilon\psi\{[(1 - B\xi^2)^{1/2}/B] + \delta\}]\}} \times \left\{\frac{[\gamma - 1)M^2(1 - B\psi^2 + 2\epsilon B\psi\delta) + 2[1 + C\psi^2 - 2\epsilon C\psi\{[(1 - B\xi^2)^{1/2}/B] + \delta\}]}{(\gamma + 1)M^2(1 - B\psi^2 + 2\epsilon\psi B\delta)}\right\}^{\gamma} \quad (10a)$$

where M is the freestream Mach number. For the singular case of a parabolic shock wave ($B = 0$, $C = 1$), the expressions for ρ,ψ,ψ_η at $\eta = 1$ and for f are

$$\rho = \frac{(\gamma + 1)M^2(1 - 2\epsilon\xi)}{(\gamma - 1)M^2(1 - 2\epsilon\xi) + 2(1 + \xi^2)}$$

$$\psi = \xi + \epsilon(\delta + \tfrac{1}{2} - \xi^2/2) \qquad \psi_\eta = \rho(\xi + \epsilon) \qquad \text{at} \quad \eta = 1 \quad (9b)$$

$$f = \frac{2\gamma M^2(1 - 2\epsilon\psi) - (\gamma - 1)[1 + \psi^2 - 2\epsilon\psi(\delta - \tfrac{1}{2} - \psi^2/2)]}{\gamma(\gamma + 1)M^2[1 + \psi^2 - 2\epsilon\psi(\delta + \tfrac{1}{2} - \psi^2/2)]} \times \left\{\frac{(\gamma - 1)M^2(1 - 2\epsilon\psi) + 2[1 + \psi^2 - 2\epsilon\psi(\delta + \tfrac{1}{2} - \psi^2/2)]}{(\gamma + 1)M^2(1 - 2\epsilon\psi)}\right\}^{\gamma} \quad (10b)$$

The boundary condition at the body is

$$\psi = 0 \qquad \text{at} \quad \eta = \eta_b \quad (11)$$

The method of solution essentially consists of separation of variables in Eqs. (8–11) by expanding the dependent variables in double McLaurin series about the shock axis of symmetry, $\xi = 0$, and about $\epsilon = 0$. Only first-order terms in ϵ are retained. This leads to ordinary differential equations with corresponding boundary conditions for unknown functions of η which can be solved only by truncating the series. The resulting equations are integrated readily by standard numerical methods. The forementioned procedure will now be carried out.

Set

$$\psi = f_{00}(\eta)\xi + f_{01}(\eta)\xi^3 + f_{02}(\eta)\xi^5 + 0(\xi^7) + \epsilon[f_{10}(\eta) + f_{11}(\eta)\xi^2 + f_{12}(\eta)\xi^4 + 0(\xi^6)] + 0(\epsilon^2) \quad (12a)$$

$$[(\gamma - 1)/(\gamma + 1)]\rho = g_{00}(\eta) + g_{01}(\eta)\xi^2 + g_{02}(\eta)\xi^4 + 0(\xi^6) + \epsilon[g_{10}(\eta)\xi + g_{11}(\eta)\xi^3 + g_{12}(\eta)\xi^5 + 0(\xi^7)] + 0(\epsilon^2) \quad (12b)$$

The first subscript on the functions of η is 0 for the zero angle of attack portion of the solution and 1 for the angle of attack portion, and the second subscript indicates the position of the term in its respective series. The forms of these expansions are ascertained readily by consideration of the initial conditions.

Expansions (12a) and (12b) are substituted into the differential Eqs. (8) and boundary conditions (9–11). Equating coefficients of like powers of ξ and ϵ results in successive problems for f_{00},g_{00}, g_{01}; $f_{00},g_{00},f_{01},g_{01},g_{02}$; etc. Thus the zero-order problem for f_{00} and g_{00} involves two equations that also contain g_{01}; the first order problem for $f_{00},g_{00},f_{01},g_{01}$ involves four equations that also contain g_{02}; and so forth. A similar pattern occurs in the successive equations for the angle-of-attack functions. This "backward influence" of g_{0n+1} in the nth-order problem is due to the ellipticity of the differential equations in the subsonic region and is a mathematical manifestation of the physical fact that disturbances are propagated in all directions in a subsonic flow. This mathematical behavior may be contrasted, for example, with that of the equations determining the coefficients of the Blasius-series solution to the parabolic equations governing the laminar boundary layer on a blunt body. Substitution of the Blasius series into the governing differential equation and equating coefficients of like powers results in equations for the series coefficients which involve only one coefficient or depend only on lower-order coefficients, and hence may be solved successively.

Now return to the problem under consideration. To solve the nth-order zero-angle problem for $f_{00},f_{01},\ldots,f_{0n}$ and $g_{00},g_{01},\ldots,g_{0n}$, some determination must be made of g_{0n+1}. The simplest thing to do is to truncate the series by setting g_{0n+1} identically equal to zero. The resulting equations may then be integrated. It is found that the differential equations for f_{00} and g_{00} are nonlinear, whereas the equations for succeeding terms in the zero-angle series are linear. The equations for all the angle-of-attack functions are linear and contain coefficients that depend on the zero-angle solution. Integration is terminated and the body shape determined by the boundary condition (11). For the angle-of-attack problem, this condition also determines δ. As an illustration of the procedure, the equations and boundary conditions for the first- and second-truncation problems for a parabolic shock wave at $M = \infty$ are presented in Ref. 9.

2. *Three-dimensional flow*

In contrast to the plane-flow case, the continuity equation is satisfied by the introduction of a pair of stream functions, ψ_1 and ψ_2, according to

$$\rho\mathbf{q} = \nabla\psi_1 \times \nabla\psi_2 \quad (13)$$

The use of such a pair of functions in this manner was introduced by Clebsch.[10]

The entropy-conservation equation, (5e), then states that

$$p/\rho^\gamma = g(\psi_1, \psi_2) \quad (14)$$

where the functional form of g is to be determined from the boundary conditions at the shock wave. Insertion of Eqs. (13) and (14) into Eqs. (5b–5d) results in coupled partial differential equations for ψ_1,ψ_2, and ρ. These equations are given in Ref. 9.

In consideration of the initial conditions at the shock wave, a few words are in order regarding the stream functions ψ_1 and ψ_2. These functions possess a degree of arbitrariness in that it is required only that the surfaces $\psi_1(\xi,\eta,\varphi) = \text{const}$ and $\psi_2(\xi,\eta,\varphi) = \text{const}$ be stream surfaces, that is, surfaces in which streamlines are imbedded. The intersections of these surfaces are then streamlines. If one considers a uniform stream for simplicity, there are any number of pairs of surfaces which can be set up to satisfy this requirement. For example, one such pair consists of orthogonal or skewed planes. Another is concentric circular cylinders and orthogonal planes through the common axis of the cylinders. If, however, one considers axisymmetric flow in a (ξ,η,φ) coordinate system and chooses for ψ_2 the azimuthal angular coordinate φ, then ψ_1 is the familiar Stokes stream function. Hence, since the small angle of attack is being considered, it is reasonable to perturb ψ_2 about φ, and ψ_1 about the Stokes function.

Consider Fig. 2. A shock wave that is a paraboloid of revolution at angle ϵ to the uniform freestream is depicted there. A line at angle ϵ through a known point on the x axis (e.g., central point of a hyperboloid, focus of a paraboloid, center

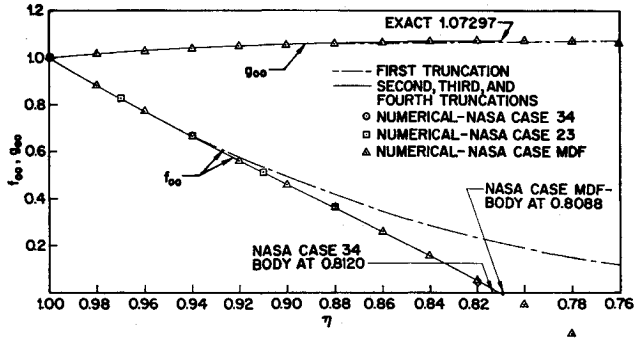

Fig. 3 Variation of reduced stream function ψ/ξ and density along the axis; circular shock, $M = \infty$, $\gamma = 1.4$

of a sphere, point of intersection of major and minor axes of an ellipsoid) is chosen as reference from which the distance to the body streamline ahead of the shock is measured. Concentric circular cylinders about $\psi_1 = 0$ and planes of angle $\beta =$ const are chosen for the stream surfaces ahead of the shock (see Sec. A-A of Fig. 2). With ψ_1 and ψ_2 defined in this manner, the initial conditions may be obtained.[9]

The boundary condition at the body is simply

$$\psi_1 = 0 \qquad \text{at } \eta = \eta_b \quad (15)$$

The method of solution is essentially the same as for plane flow. Separate variables by setting

$$2\psi_1 = f_{00}(\eta)\xi^2 + f_{01}(\eta)\xi^4 + f_{02}(\eta)\xi^6 + 0(\xi^8) + \epsilon\cos\varphi[f_{10}(\eta)\xi + f_{11}(\eta)\xi^3 + f_{12}(\eta)\xi^5 + 0(\xi^7)] + 0(\epsilon)^2 \quad (16a)$$

$$\psi_2 = \varphi + \epsilon\sin\varphi\{[h_{10}(\eta)/\xi] + h_{11}(\eta)\xi + h_{12}(\eta)\xi^3 + 0(\xi^5)\} + 0(\epsilon^2) \quad (16b)$$

$$[(\gamma-1)/(\gamma+1)]\rho = g_{00}(\eta) + g_{01}(\eta)\xi^2 + g_{02}(\eta)\xi^4 + 0(\xi^6) + \epsilon\cos\varphi[g_{10}(\eta)\xi + g_{11}(\eta)\xi^3 + g_{12}(\eta)\xi^5 + 0(\xi^7)] + 0(\epsilon^2) \quad (16c)$$

Again, after one substitutes these expansions into the governing equations and boundary conditions and equates coefficients of like powers of ξ and ϵ, the series must be truncated to obtain a solution. As in the plane-flow case, the equations for f_{00} and g_{00} are nonlinear, and succeeding equations for the other unknown functions of η are linear, with the equations for the angle-of-attack functions having variable coefficients depending on the zero-angle solution. The body boundary condition, Eq. (15), is applied in a similar manner as outlined for plane flow.[9]

3. *Sonic lines and surface pressure distributions*

In addition to body shapes, sonic lines and surface pressure distributions out to the sonic line were calculated to investigate convergence of the series expansions away from the axis. The mathematical details of obtaining these quantities will now be presented.

The energy-conservation equation for a perfect gas may be written as

$$\frac{\gamma}{\gamma-1}\frac{\bar{p}}{\bar{\rho}} + \frac{\bar{q}^2}{2} = \frac{\gamma}{\gamma-1}\frac{\bar{p}_\infty}{\bar{\rho}_\infty} + \frac{\bar{q}_\infty{}^2}{2} \quad (17)$$

where barred quantities represent dimensional physical quantities. This becomes, after suitable nondimensionalization,

$$M_l{}^2 = \frac{2}{\gamma-1}\left[\frac{2+(\gamma-1)M^2}{2\gamma M^2}\frac{\rho}{p} - 1\right] \quad (18)$$

where M_l is the local Mach number of the flow in the shock layer. On the sonic line, the local Mach number is unity. Furthermore, the mass- and entropy-conservation equations yield $p = \rho^\gamma f(\psi)$ (plane flow) and $p = \rho^\gamma g(\psi_1,\psi_2)$ (three-dimensional flow). Putting this information into Eq. (18) yields

$$\frac{2+(\gamma-1)M^2}{2\gamma M^2}\frac{\rho^{1-\gamma}}{f(\psi)} = \frac{\gamma+1}{2} \qquad (\nu = 0) \quad (19a)$$

$$\frac{2+(\gamma-1)M^2}{2\gamma M^2}\frac{\rho^{\gamma+1}}{g(\psi_1,\psi_2)} = \frac{\gamma+1}{2} \qquad (\nu = 1) \quad (19b)$$

Introduction of f or g in terms of the series expansions for ψ, ψ_1, and ψ_2 yields equations that, for a given truncation, are algebraic expressions for ξ in terms of functions of η. Selection of values of η between the shock and body allows corresponding values of ξ to be calculated, thus determining points on the sonic line.

The equations for surface pressure distributions are obtained by using

$$p = \rho^\gamma f(\psi) \qquad (\nu = 0) \quad (7)$$

$$p = \rho^\gamma g(\psi_1,\psi_2) \qquad (\nu = 1) \quad (14)$$

Again, substituting appropriate expansions for ρ, f, and g yields $p(\xi,\eta,\nu\varphi;\epsilon)$. Use of known values of ξ,η and $\nu\varphi$ on the body allows the pressure to be calculated in any given truncation.

III. Results and Discussion

A. Infinite Mach Number

1. *Zero angle of attack*

To examine the convergence of the series expansions for the stream functions and density, zero-angle-of-attack results will be presented initially. From consideration of the simplifications brought about in the equations and boundary conditions, the freestream Mach number is taken to be infinite and the shock shape to be a portion of a circle and a parabola. Bodies supporting shock waves that are portions of a sphere and paraboloid of revolution are considered also in Ref. 9. The specific heat ratio γ is taken to be 1.4.

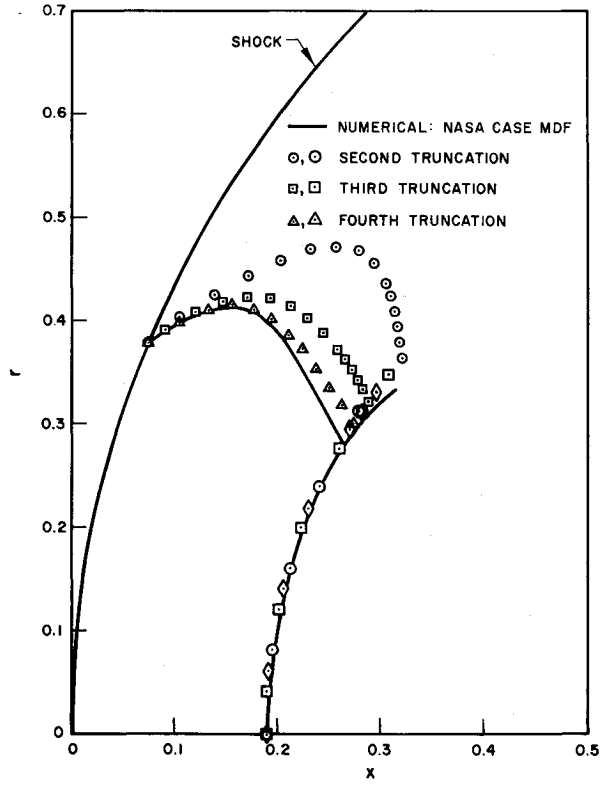

Fig. 4 Comparison of body shapes and sonic lines; circular shock, $M = \infty$, $\gamma = 1.4$

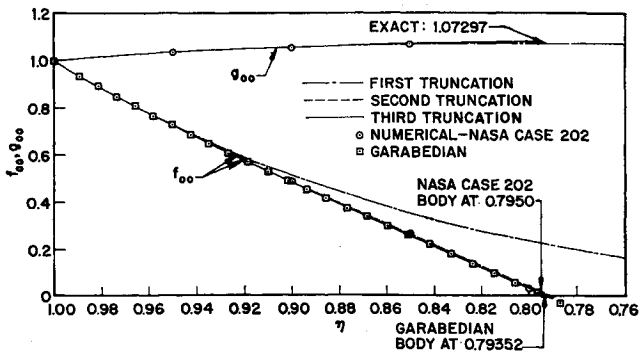

Fig. 5 Variation of reduced stream function ψ/ξ and density along the axis; parabolic shock, $M = \infty$, $\gamma = 1.4$

The first four truncation problems have been solved for the circular shock, whereas the first three truncation problems have been calculated for the parabolic shock wave. The numerical integration of the ordinary differential equations for the unknown functions of η was accomplished using a fourth-order Runge-Kutta-Gill method.[11] The computations were carried out on an IBM 7090 electronic computing machine at Lockheed Missiles and Space Company, Sunnyvale, Calif. Machine times of 2 to 3 min were required for each case.

Results on and away from the axis are compared with numerical solutions obtained using the inverse method developed by Van Dyke[1] and refined by Fuller.[12] Convergence on the axis is extremely rapid, truncation at three terms giving the stagnation-point density correct to five significant figures and the standoff distance to four significant figures as determined by comparison of the parabolic shock solution with Garabedian's results.[13] Convergence away from the axis is somewhat less rapid, as is to be expected from the form of the expansions. The term convergence is used here in the sense that, whenever two successive truncation solutions yield values for a physical quantity identical in three or more significant figures, it is said that the quantity has converged. Nothing can be said about convergence of the assumed series in the strict mathematical sense, since the functional form of the series coefficients is not known explicitly.

Results for the circular and parabolic shock waves are given in Figs. 3–6. Figures 3 and 4 apply to the circular shock. In Fig. 3, the convergence of the reduced stream function ψ/ξ and the density function $(\gamma - 1)\rho/(\gamma + 1)$ along the axis ($\xi = 0$) is examined, and the results of truncating the series for ψ and ρ at one, two, three, and four terms are compared with numerical solutions. As previously mentioned, convergence is extremely rapid for both the density and stream function, the differences between the second, third, and fourth truncations being indiscernible to the scale of the plot. The standoff distance referred to the shock nose radius Δ/R_s is determined to be 0.1895 by the second truncation and 0.1899 by the third and fourth truncations. This converged result is smaller than the value of 0.1912 determined by NASA case MDF† and larger than the value of 0.1880 determined by NASA case 34. [These values for standoff distance are obtained using that value of η at which f_{00} goes to zero, along with Eq. (2*d*).] The method of solution for NASA case MDF contains a smoothing process,[12] whereas that for case 34 does not. As pointed out in Ref. 12, the smoothing process has the effect of increasing standoff distance. Comparison of the two NASA results with the converged value leads to the conclusion that the NASA data are not sufficiently accurate to be used as an absolute basis of comparison. This point will be borne out further as other physical quantities are considered.

Figure 4 compares sonic lines and body shapes as determined from the second, third, and fourth truncations with the results

† NASA results for cases MDF, MDD, RS1, and RS4 are the courtesy of Ames Aeronautical Laboratory (unpublished).

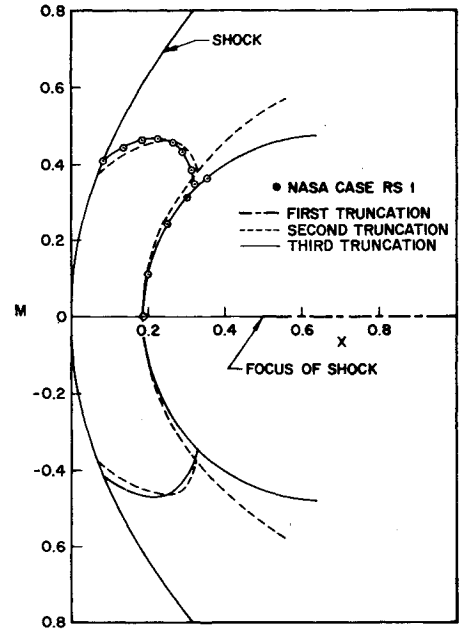

Fig. 6 Body shapes and sonic lines; parabolic shock, $M = \infty$, $\gamma = 1.4$, $\epsilon = 0°$

of NASA case MDF. The sonic line determined by the first truncation is a circle having a radius of 1.593 and center at $x = 1$, $r = 0$, whereas the first-truncation body determined by the numerical integration is the point $x = 1$, $r = 0$. Note that the first-truncation sonic line lies ahead of the shock. This result is obtained by analytic continuation of the solution upstream of the shock wave and is, of course, physically unrealizable, since the flow ahead of the shock is uniform at infinite Mach number. Comparison of the body shapes determined by truncating the series at three and four terms indicates convergence beyond the sonic point to a shape other than the NASA result. The sonic line, however, has not converged, and retention of higher-order terms would be required to determine its exact location.

Figures 5 and 6 apply to a parabolic shock. The results of truncation at one, two, and three terms for the reduced stream function and density function along the axis are compared with both NASA results and Garabedian's solution[13] in Fig. 5. Results for the circular shock have indicated that the NASA data lack sufficient accuracy to be used as an absolute basis for comparison and that the method under consideration possesses internal consistency. The question of convergence to the correct solution may be answered by comparison with Garabedian's result for a parabolic shock at infinite freestream Mach number. Garabedian claims 0.1% accuracy for his standoff distance of 0.18516. Truncation at three terms yields a standoff distance of 0.18514, thus indicating at least three, and perhaps four, significant-figure accuracy for this quantity.

Figure 6 compares body shape and sonic lines as determined by truncation at one, two, and three terms with NASA results. For this case, comparison indicates near convergence of the third truncation result for both quantities.

2. *Small angle of attack*

The analysis outlined for the angle-of-attack problem has been carried out for shock waves that are parabolas (plane flow) and paraboloids of revolution (three-dimensional flow). The first three truncation problems have been solved for each shock shape. The freestream Mach number is taken to be infinite, and γ takes on the values 1.4, 1.2, 1.1, 1.05. The resulting body shapes, sonic lines, and positions of the body streamlines at their points of intersection with the shock wave are shown in Figs. 7 and 8 for $\epsilon = 10°$, $\gamma = 1.4$, where a finite value of ϵ has been selected for graphical purposes and the

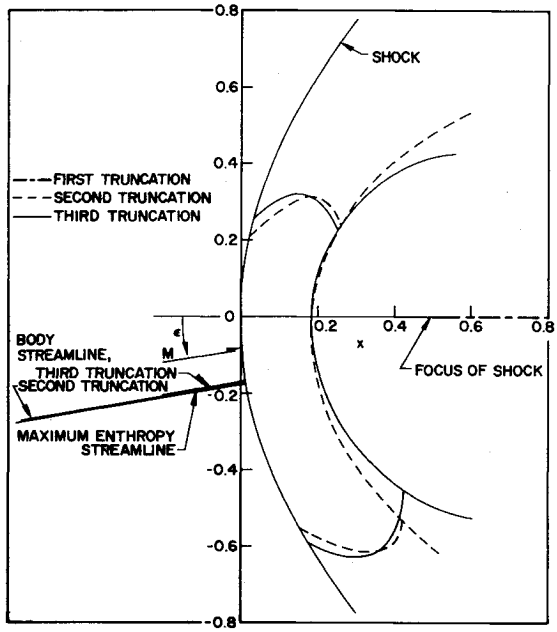

Fig. 7 Body shapes, sonic lines, and comparison of body streamlines with maximum entropy streamline; parabolic shock, $M = \infty$, $\gamma = 1.4$, $\epsilon = 10°$

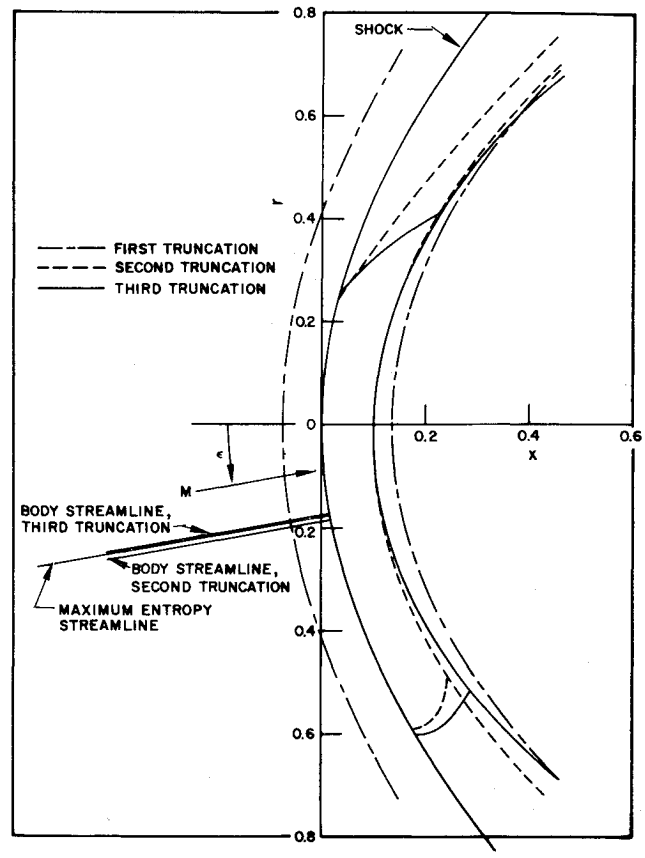

Fig. 8 Body shapes, sonic lines, and comparison of body streamlines with maximum entropy streamline; paraboloidal shock, $M = \infty$, $\gamma = 1.4$, $\epsilon = 10°$

error is $0(\epsilon^2)$. For purpose of comparison, body shapes and sonic lines for a parabolic shock at zero angle are given in Fig. 6. Computing machine times of 5 to 6 min per case were required since the zero-angle functions appear as coefficients in the angle-of-attack equations and hence must be stored in the machine. Also, in certain cases, it was necessary to use very small step sizes (e.g., $\Delta\eta = 10^{-4}$) in order to obtain accurate values for the quantity δ.

Of particular interest in the angle-of-attack problem is whether or not the streamline that wets the body crosses the shock normally, thus having maximum entropy. For this to be so, the quantity δ (see Fig. 2) must have the value $\frac{1}{2}$. The results of the analyses are given in Table 1.

For all cases the trend of decreasing δ with increasing truncation is toward a value of δ slightly less than $\frac{1}{2}$. For the three-dimensional case, a reversal of this trend in higher truncations conceivably could result in a value of $\frac{1}{2}$. However, even if this reversal took place in two dimensions, a converged value would be expected to lie between the second- and third-truncation values and thus never could be $\frac{1}{2}$. Hence, the streamline that wets the body passes through the shock wave slightly above the point where it is a normal shock. However, as the Newtonian limit process ($M \to \infty$, $\gamma \to 1$) is carried out, the trend is toward a value of $\frac{1}{2}$. Hence, in this limit, when the parabolic and paraboloidal shock and body coincide, the body is covered by the maximum-entropy streamline in both the plane and three-dimensional cases.

Since the shock waves possess symmetry about the x axis, the resulting body shapes are asymmetric to this axis. Consideration of the comparison in Fig. 6 of the third-truncation body for the parabolic shock at zero angle with the NASA results and of the results for the circular shock given in Fig. 4 leads to the conclusion that, for symmetric plane flow at $M = \infty$, truncation at three terms yields a nearly converged body out to the sonic point. Since ϵ is taken as small, it is reasonable to extend this conclusion to include small angles of incidence. With these facts in mind, and the realization that it is somewhat impractical to talk about asymmetric shapes from an experimental or engineering viewpoint, an attempt was made to find an axis system in which that portion of the two-dimensional body given by the third truncation (Fig. 7) out to the sonic points could be approximated closely by a conic section. An ellipse was fitted by a trial-and-error procedure in which the positions of the foci and major axis were varied until points on the ellipse and third-truncation body coincided to three significant figures.[9] The ellipse is given by the equation $\bar{x}^2/0.37 + \bar{r}^2/0.28 = 1$, where the origin of the $(\bar{x}, \bar{r})$ axes is at $x = 0.790$, $r = -0.033$, and the $\bar{x}$ axis is at angle 14.20° measured clockwise from the freestream direction. Thus, the shock wave is seen to rotate about 70% as fast as the body as the angle of attack is imposed.

B. Finite Mach Number, Zero Angle of Attack

The truncation method of solving hypersonic blunt-body flows in the subsonic region between the shock wave and body converges fairly rapidly when the freestream Mach number is infinite. To investigate the behavior of the method at finite Mach numbers, specific cases were chosen where comparison could be made with experimental results and other theoretical solutions.

Table 1 Values of δ

	Parabolic Shock, $M = \infty$				Paraboloidal shock, $M = \infty$			
	γ				γ			
Truncation	1.4	1.2	1.1	1.05	1.4	1.2	1.1	1.05
1	1518.0	8417.0	...	...	88.00	37.48	25.79	−1.34
2	0.4838	0.4935	0.4974	0.4990	0.5576	0.5394	0.5190	0.5042
3	0.4768	0.4908	0.4966	0.4988	0.4871	0.4950	0.4984	0.5004

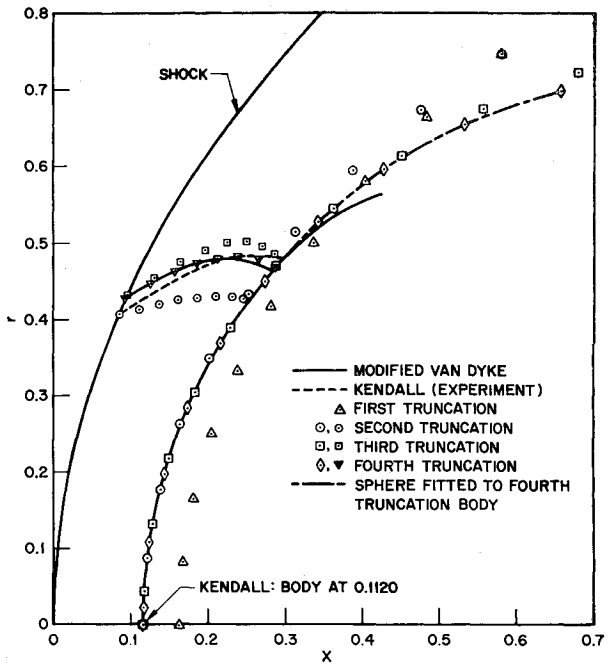

Fig. 9 Comparison of body shapes and sonic lines; spherical body, $M = 4.76$, $\gamma = 1.4$

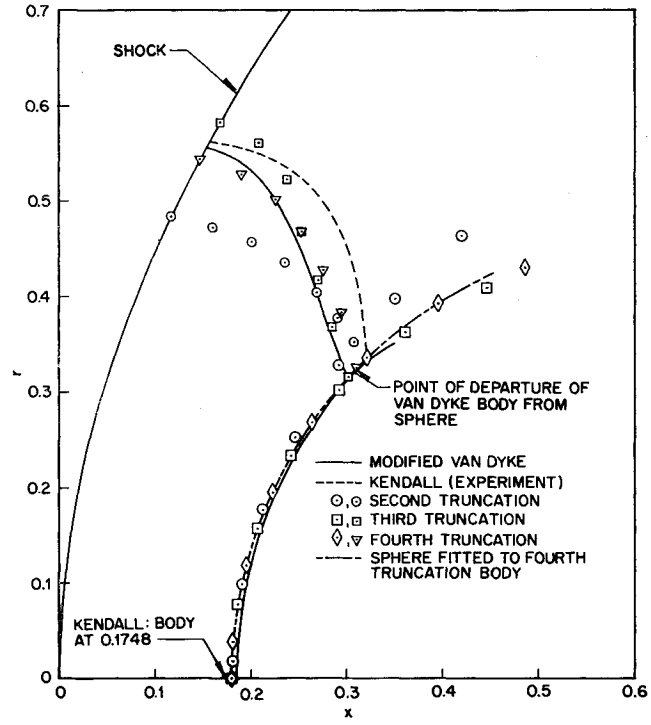

Fig. 10 Comparison of body shapes and sonic lines; spherical body, $M = 1.85$, $\gamma = 1.4$

Results are presented for spherical bodies at $M = 4.76$ and 1.85 in Figs. 9 and 10 and are compared with experimental data of Kendall,[14] and theoretical solutions are obtained using the modified Van Dyke method[12] for axisymmetric flow. Figure 11 compares the solutions generated by a hyperbolic shock wave at $M = 5.8$ with results obtained by Garabedian and Lieberstein[15] and by the modified method of Van Dyke. Figure 12 compares body shapes and sonic lines for flow at $M = 4.0$ about an oblate ellipsoid of revolution having an axis ratio of 3 to 2 with results of the direct method of Belotserkovskii[16] and the modified Van Dyke method.

Solutions to the problems that result when the series expansions for the stream function and density are truncated at one, two, three, and four terms are presented for the sphere at $M = 4.76$. However, since the first-truncation results are known qualitatively (body an $\eta = \text{const}$ line, sonic line ahead of the shock, surface pressure constant at the stagnation value), they are not included in the results at $M = 1.85$, 5.8, and 4.0. The second-, third-, and fourth-truncation problem solutions are presented for these cases.

Figure 9 compares body shapes and sonic lines for the $M = 4.76$ case. Note that the body shape is converged well beyond the sonic point in the third truncation and that the fourth truncation yields nearly a hemisphere, whereas the body obtained by the modified Van Dyke method departs sharply from a sphere just beyond the sonic point. Recall that similar behavior of the Van Dyke solutions was observed in the $M = \infty$ cases. Further note the good agreement among the fourth-truncation sonic line and the experimental and Van Dyke sonic lines.

Since the Mach number terms in the differential equations and boundary conditions are $0(1/M^2)$, calculations at $M = 4.76$ do not provide a very severe test for the truncation method. Hence, an attempt was made to obtain a sphere at $M = 1.85$. Figure 10 shows the resulting body shapes and sonic lines determined from the second-, third-, and fourth-truncation problems and compares them with the results of Van Dyke and Kendall. Worthy of attention in this figure are three things. First, note the large differences in standoff distances given by the three results and that the standoff distance obtained by the truncation method is closer to the experimental value than is that of the Van Dyke method. Second, note that the fourth-truncation body is a sphere for greater distance beyond the sonic point than is the Van Dyke body. (This apparent superiority of the truncation method over that of Van Dyke may, of course, be of little practical significance, since the body shape downstream of the last point from which the left running characteristic intersects the sonic line has no effect on the subsonic flow.) Third, note the sonic lines and the fact that the fourth-truncation line more nearly parallels the experimental sonic line than the Van Dyke result.

Figure 11 compares body shapes and sonic lines with the results of Garabedian and Lieberstein and Van Dyke. There is close agreement for both quantities among the fourth-truncation results and those to which they are being compared.

Figure 12 compares body shapes and sonic lines with results of the modified Van Dyke method and the direct method of Belotserkovskii. To the scale of the plot, the shock waves necessary to produce the 3:2 ellipsoid by the fourth-truncation and Van Dyke methods are identical to those obtained by Belotserkovskii up to a substantial distance beyond the sonic line. However, the Van Dyke body deviates (to the scale of the plot) from a 3:2 ellipsoid before the sonic point is reached, and the fourth-truncation sonic line shows closer agreement with that of Belotserkovskii than does the sonic line obtained by the Van Dyke method.

IV. Conclusions

A semi-analytical, semi-numerical method of analysis has been developed and successfully applied to the problem of two- and three-dimensional hypersonic flow past blunt bodies at small angles of attack.

Solutions at zero angle of attack are obtained as a special case of the general problem. Standoff distances are predicted to higher accuracy than by any other existing method in popular use.

For a shock wave that is a parabola or paraboloid of revolution at angle of incidence to a uniform freestream having infinite Mach number and $\gamma = 1.4$, the streamline that wets the body passes through the shock wave slightly above the point where it is a normal shock wave. Hence, the body is not covered by the maximum-entropy streamline in these cases. In the Newtonian limit ($M = \infty$, $\gamma = 1$), the parabolic or

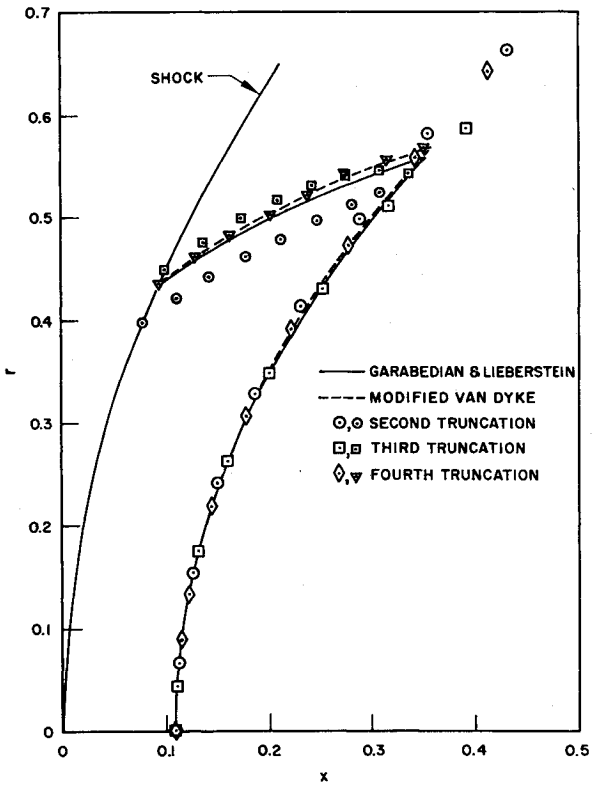

Fig. 11 Comparison of body shapes and sonic lines; $B = 1/(M^2 - 1)$, $\nu = 1.0$, $M = 5.8$, $\gamma = 1.4$

paraboloidal body is wetted by the maximum-entropy streamline. For a parabolic shock at infinite Mach number, $\gamma = 1.4$, the shock wave rotates more slowly than the body as angle of attack is imposed.

References

[1] Van Dyke, M. D., "The supersonic blunt-body problem—review and extension," J. Aerospace Sci. **25**, 485–496 (1958).

[2] Hayes, W. D. and Probstein, R. F., *Hypersonic Flow Theory* (Academic Press Inc., New York, 1959), pp. 150–230.

[3] Van Dyke, M. D. and Gordon, H. D., "Supersonic flow past a family of blunt axisymmetric bodies," NASA TR R-1 (1959).

[4] Belotserkovskii, O. M., "On the calculation of flow past axisymmetric bodies with detached shock waves using an electronic computing machine," Prikl. Mat. Mekh. **24**, no. 1, 511–517 (1960).

[5] Mangler, K. W., "The calculation of the flow field between a blunt body and the bow wave," *Hypersonic Flow* (Butterworths Scientific Publications, London, 1960), pp. 219–239.

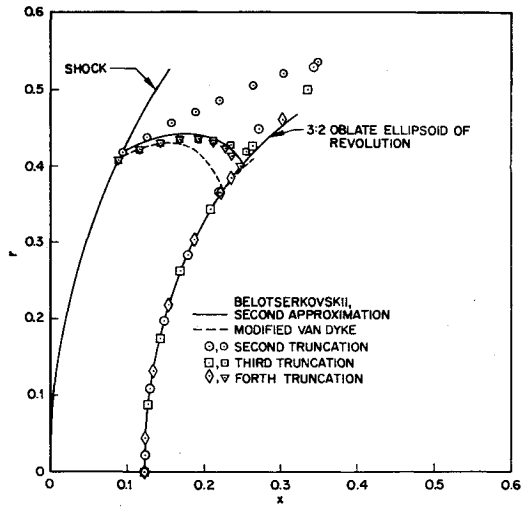

Fig. 12 Comparison of body shapes and sonic lines; 3:2 oblate ellipsoidal body, $M = 4.0$, $\gamma = 1.4$

[6] Vaglio-Laurin, R. and Ferri, A., "Theoretical investigation of the flow field about blunt-nozed bodies in supersonic flight," J. Aerospace Sci. **25**, 761–770 (1958).

[7] Vaglio-Laurin, R., "On the PLK method and the supersonic blunt body problem," IAS Preprint 61-22 (January 1961).

[8] Ames Research Staff, "Equations, tables, and charts for compressible flow," NACA Rept. 1135 (1953).

[9] Swigart, R. J., "A theory of asymmetric hypersonic blunt-body flows," Stanford Univ. Dept. Aeronaut. Astronaut. Rept. 120 (January 1962).

[10] Clebsch, A., "Ueber Eine Allgemeine Transformation der Hydrodynamischen Gleichungen," Crelle **54**, 303 (1857).

[11] Gill, S., "A process for the step-by-step integration of differential equations in an automatic digital computing machine," Proc. Cambridge Phil. Soc. **47**, 96–108 (January 1951).

[12] Fuller, F. B., "Numerical solutions for supersonic flow of an ideal gas around blunt two-dimensional bodies," NASA TN D-791 (July 1961).

[13] Garabedian, P. R., "Numerical construction of detached shock waves," J. Math. Phys. **36**, 192–205 (1957).

[14] Kendall, J. M., Jr., "Experiments on supersonic-blunt-body flows," Jet Propulsion Lab. Progr. Rept. 20-372 (1959).

[15] Garabedian, P. R. and Lieberstein, H. M., "On the numerical calculation of detached bow shock waves in hypersonic flow," J. Aeronaut. Sci. **25**, 109–118 (1958).

[16] Belotserkovskii, O. M., "Calculation of flow past axisymmetric bodies with detached shock waves (equations and tabulated flow fields)," Computing Center Rept., Academy of Sciences, USSR, Moscow (1961).

[17] Vaglio-Laurin, R., private communication (November–December 1961).